Chapter 13
Numerical Treatment of Multidimensional Stochastic, Competitive and Evolutionary Models

Mostafa Zahri

Abstract In this chapter, we present a computational study of multi-dimensional stochastic systems of differential equations. Especially competitive and evolutionary models. In these types of models, a certain number of uncertainties are causing side effects as random excitations and interactions. To numerically solve the considered systems, we propose the Itô-Taylor family schemes for multi-dimensional stochastic differential equations. Either for systems driven by one white noise or for systems having more than one source of excitations. A first-order accuracy is ensured in the approximation of double Itô integrals by using a truncation in the Fourier series expansion. To verify the accuracy of the proposed method, we consider a system of two stochastic differential equations with known analytical solution. Numerical results are presented for a reduced prototype system of the prebiotic evolutionary model.

13.1 Introduction

After the discovery of the catalytic process of some RNA-like molecules (ribozymes) [7], the formation of prebiotic material has been subject of many theoretical an experimental studies, see [4] among others. These RNA-like molecules (also referred to as replicators) with unspecific catalytic capabilities could have formed ensemble of species, the so-called catalytic networks. It should be pointed out that, although the evolution of these catalytic networks has been extensively studied from a theoretical point of view over the last decades, most of the work has been focused on the analysis of their dynamics under deterministic input conditions [11]. Less attention has been given to the role of stochastic excitations on the behavior of these prebiotic models. However, it is well known that stochastic forces may play an important role on the dy-

M. Zahri (✉)
College of Sciences, University of Sharjah, Sharjah, UAE
e-mail: mzahri@sharjah.ac.ae

A. Boutayeb (ed.), *Disease Prevention and Health Promotion in Developing Countries*,
https://doi.org/10.1007/978-3-030-34702-4_13

namics of the biochemical systems. For instance, the stochastic forces may probably occur in the reaction medium known by the prebiotic soup, see [8, 9] for more details. Therefore, it ought to be taken into account in the mathematical equations governing these models. In this chapter, we consider the problem of prebiotic evolution in one of the theoretical models proposed to study the behavior of catalytic networks [15]. This model is a closed system (only energy can be interchanged with the surroundings) where activated material (nucleotides) react to build up self-replicative units following preestablished rules. These energy rich monomers are regenerated from the by-product of the reaction (obtained mainly as the result of the hydrolysis of self-replicative species) by means of a recycle mechanism (basically due to an external energy source, for example sunlight). The closure of the system directly imposes a selection pressure on the population. All these biochemical features can be mathematically modeled by a multi-dimensional system of deterministic ordinary differential equations with nonlinear kinetic reactions, see for example [9, 15]. The spatial effects can also be incorporated into this model by introducing the diffusion operator in the ordinary differential equations resulting in a set of reaction-diffusion equations, compare [4]. To stabilize these partial differential equations, authors in [36, 44, 46] have added an additive noise into the system. In the present work, we propose a new technique to account for excitations from the prebiotic medium. The key idea is to introduce a stochastic diffusion matrix in the system of ordinary differential equations and transform this model to a system of stochastic differential equations. Here, we consider a drift term driven by both additive and multiplicative noises and it can be raised from uncertainties in catalytic coefficients or simply by excitations from the prebiotic medium. The main advantage of such approach comes from the fact that features of interest in random dynamics (i.e. random fixed points, random bifurcation, random attractors, etc.) are harder to describe in the framework of stochastic calculus than in the framework of classical deterministic calculus.

To numerically approximate the solutions of the proposed systems, we apply a generalized Milstein method [20–22, 26]. The basic ingredients of this approach are the piecewise linear approximation by the Itô-Taylor expansion of the vector fields and the numerical integration of the resulting linear equation. Fourier series expansions are used to approximate double Itô integrals. In the case of stochastic differential equations, the Milstein method has been restricted either to the class of equations with additive noise terms or scalar equations with multiplicative noise. Therefore, the application of the Milstein method to cover wider classes of stochastic differential equations is an appealing challenge. In particular, the current study focuses in the class of stochastic differential equations driven by multiplicative noise. Numerical results are presented for a prototype system of four catalyzed self-replicator species along with activated and inactivated residues. Phase-space portraits and strange attractors are also displayed. In the same context, Stochastic partial differential equations (SPDEs) are essentially partial differential equations with additive or multiplicative noise and random forcing parameters. Generally, solving SPDEs either analytically or numerically is not an easy task. However, in the last few years there was a growing interest to model interesting applications in hydrodynamics, quantum field theory, engineering and statistical mechanics by using time-space evolutionary models with

non deterministic excitations [2, 5, 12]. Recently, the numerical approximation of sample solutions of such stochastic models has attracted more attention in several studies [18, 27, 28, 46, 47]. The presence of different sources of uncertainties in the form of dependent and independent stochastic processes brings more complexity to this topic. For instance, the fluid transport phenomena occurs through several physical and chemical combinations of reactions, diffusions and advections. It demonstrates a significant part of oceanography and involves an interesting interpretation of the geochemical distributions in the water [3, 6]. All these factors contain some levels of random excitations, their numerical treatment leads to the space time integration of SPDEs [13, 31]. The treatment, separation or distillation of these homogeneous or nonhomogeneous substance concentration could be a challenge for an engineering work.

In the works [29, 35, 36], we were focused more on implementing deterministic techniques for stochastic time-space integration of different SPDEs with different physical or biological meanings. For instance, we studied the stochastic method of lines for solving boundary value problems [46, 47]. In [24], we analyzed and implemented the Wick-product techniques for solving reaction-diffusion problems. However, the common point that we have remarked was, on the one hand the expensive computational cost and on the other hand the non trivial construction of effective high order methods. Where approximation of multiple stochastic integrals in the Itô sense are required. In the present work, we combine three methods, namely the method of lines (MOL) [37, 41, 42], the domain-decomposition method (DDM) for non-overlapping subdomains [23, 25, 33, 34] and the Itô-Taylor schemes for stochastic differential equation [20–22]. Moreover, we have to mention that the major difficulties in using the domain-decomposition methods is the determination of the interface solution and connecting it with the interior solution into an accurate approximation. It is side effect of dividing the problem into subproblems, so one can approximate the parts of the solution with significant independence of the other parts either by using overlapping or non-overlapping subdomains. To complete the suggested method, we introduce the barycenter interpolation method (BIM) for approximating the missing concentration values on the interfaces connecting the subdomains. The treatment of the non local behaviors of physical and biological systems are reasonable motivations for the use of DDM, which are characterized by the referred parallelization advantages or the discretization of domains with complex geometries [14, 38–40].

Although in the last years several theoretical techniques for the numerical and computational treatment for SPDEs has been developed [1, 30]. However, implementing high order accurate methods is still an interesting and relevant task. It is important to note that there exists no explicit Itô-Taylor formula for SPDEs [18]. Therefore, the use of deterministic classical methods for solving SPDEs is generally non-trivial, for more details see [45].

13.2 Stochastic Model for Prebiotic Evolution

The model we consider in this paper consists on the replication of N reacting species $I_1, I_2, \ldots, I_N$ using activated monomers A and inactivated residues B according to the following reactions:

$$I_i + A \xrightarrow{\alpha_i} 2I_i, \qquad \text{(R1)}$$

$$I_i + I_j + A \xrightarrow{k_{ji}} 2I_i + I_j, \qquad \text{(R2)}$$

$$I_i \xrightarrow{\delta_i} B, \qquad \text{(R3)}$$

$$B \xrightarrow{\gamma} A. \qquad \text{(R4)}$$

These reaction steps have been used in pattern formation in a model proposed to study the behavior of catalytic networks in the RNA-like molecules, compare [4, 11, 32] among others. This notation is intended to be similar to that used in traditional chemistry for which the steps (R1)–(R2) mean:

(R1) Each specie I_i ($i = 1, \ldots, N$), in the presence of the substrate A, selfreplicates noncatalytically with a rate α_i.
(R2) Specie I_j ($j \neq i$) catalyzes the selfreplication of the species I_i with a rate k_{ji} in the presence of the substrate A.
(R3) Specie I_i degrades in B with a rate δ_i.
(R4) The product of the degradation B is recyclated in energy-high substrate A with a rate γ.

For more details on biochemical aspects of the considered model we refer the reader to [4, 11, 32] and further references are cited therein. The above set of reactions can be mathematically formulated based on deterministic ordinary differential equations (ODE). Thus, if we use the notation x_i, y and z to denote respectively, the concentrations of the selfreplicator species I_i, the activated monomers A and the inactivated residues B then the reactions (R1)–(R4) are modelled by the following deterministic system of ODE

$$\begin{aligned}
\frac{dx_j}{dt} &= x_j \left(y \left(\alpha_j + \sum_{i=1}^{N} k_{ij} x_i \right) - \delta_j \right), \qquad j = 1, \ldots, N, \\
\frac{dy}{dt} &= \gamma z - \left(y \left(\sum_{i=1}^{N} \alpha_i x_i + \sum_{i=1}^{N} \sum_{j=1}^{N} k_{ij} x_i x_j \right) \right), \\
\frac{dz}{dt} &= \sum_{i=1}^{N} \delta_i x_i - \gamma z,
\end{aligned} \qquad (13.1)$$

where the concentrations $x_j(t)$, $y(t)$ and $z(t)$ are functions of time variable in a time interval $[t_0, T]$ with t_0 and T are the initial and final times, respectively. It is easy to remark that the system (13.1) verifies

$$\sum_{j=1}^{N} x_j + y + z = c,$$

with c being the total concentration of the prebiotic model. The deterministic system (13.1) has been analyzed in [32] and numerical simulations are included therein. In this reference, no effects from the prebiotic medium have been accounted for in the governing equations. However, medium effects can strongly interact with kinetic reactions and neglecting medium effects may have significant consequences in the overall predictions. In order to incorporate the medium effects in the system (13.1), the authors in [4] have introduce the spatial dependence of the concentrations x_i, y and z. Thus, the ODE system (13.1) is transformed to a deterministic system of partial differential equations (PDE) of reaction-diffusion type. A stochastic counterpart of this PDE system was also investigated in [36, 44].

In the present study, to account for medium effects in the prebiotic evolution model we propose random perturbations in the kinetic reactions (13.1). Hence, the system (13.1) is transformed to a set of stochastic differential equations (SDE) of the following form

$$\begin{aligned}
dx_j &= \left(x_j \left(y \left(\alpha_j + \sum_{i=1}^{N} k_{ij} x_i \right) - \delta_j \right) \right) dt + \sigma_j dW_j, \qquad j = 1, \ldots, N, \\
dy &= \left(\gamma z - \left(y \left(\sum_{i=1}^{N} \alpha_i x_i + \sum_{i=1}^{N} \sum_{j=1}^{N} k_{ij} x_i x_j \right) \right) \right) dt + \sigma dW, \\
dz &= \left(\sum_{i=1}^{N} \delta_i x_i - \gamma z \right) dt + \sigma dW,
\end{aligned} \tag{13.2}$$

where $\sigma_j = \sigma_j(x_1, \ldots, x_N, y, z)$ and $\sigma = \sigma(x_1, \ldots, x_N, y, z)$ are perturbation coefficients, W_i and W are Wiener processes. Note that σ_j and σ may be interpreted as a dimensional parameter that scales the diffusion process. In the framework of stochastic differential equations, the Eqs. (13.2) should be interpreted as

$$d\mathbf{X}(t) = \mathcal{F}(t, \mathbf{X}(t))dt + \mathcal{G}(t, \mathbf{X}(t))d\mathbf{W}(t), \qquad \mathbf{X}(t_0) = \mathbf{X}_0, \tag{13.3}$$

where $\mathbf{X} = (x_1, \ldots, x_N, y, z)^T$ is the $(N+2)$-vector of the unknown concentrations, $\mathcal{F}(t, \mathbf{X}(t))$ is the $(N+2)$-vector of the kinetic reactions known as drift vector, $\mathcal{G}(t, \mathbf{X}(t))$ is the $(N+2) \times d$-matrix known by diffusion matrix, $\mathbf{W}(t)$ is a d-vector

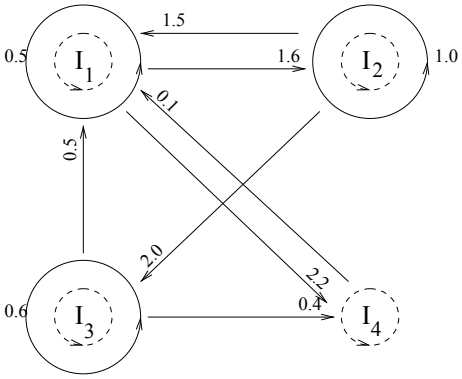

Fig. 13.1 The reduced prototype system used for numerical simulations

Wiener process, and $\mathbf{X}_0$ is a $(N+2)$-vector of the initial conditions given at time t_0. Here, each entry of the d-vector $\mathbf{W}(t)$ forms a Brownian motion which is independent of the other elements.

Note that the model (13.2) is formed by $(N+2)$ coupled SDE with nonlinear reaction terms and stochastic excitations caused by the prebiotic medium. In our numerical results, we have used a reduced prototype system of four catalyzed selfreplicator species along with activated and inactivated residues depicted in Fig. 13.1. The numbers shown in the arrows of this figure refer to the catalytic rates k_{ji}, $1 \leq i, j \leq 4$ appeared in (13.2).

13.3 Itô Taylor Scheme for Multi-dimensional Stochastic Systems

One of the main concerns of the Stochastic Calculus is the new concept of differentiability. For instance, we know that the path of a Brownian motion is continuous but nowhere differentiable and in order to define a stochastic differential equation and integrals, we have to introduce the notion of stochastic differentiability. The central result is the Itô-Formula, which leads to a new definition of differential equation and a new concept of Taylor expansion.

13.3.1 Higher Order Itô-Formula for Stochastic Differentiation

A process satisfying a stochastic differential equation (SDE) in the sense of Itô, see [16, 17], will be called an Itô process.

Definition 13.1 Let $(W_t)_{t\in\mathbb{T}}$ be an m-dimensional Brownian motion defined on a $(\Omega, \mathfrak{A})^m$ with right continuous augmented filtration $\mathfrak{F} = (\mathfrak{F}_t)_{t\in\mathbb{T}}$. The process $(X_t^1 \ldots, X_t^d)$ is called Itô Processes, if and only if it has the following form

$$X_t^i = X_{t_0}^i + \int_{t_0}^t a_s^i ds + \sum_{j=1}^m \int_{t_0}^t b_s^{i,j} dW_s^j; \qquad i = 1, \ldots, d; \quad j = 1, \ldots, m \tag{13.4}$$

where for all i, j; $(a_t^i)_{t\in\mathbb{T}}$, $(b_t^{i,j})_{t\in\mathbb{T}}$ are $\mathfrak{F}_t$ adapted, $\int_{t_0}^T a_s^i ds < \infty$ and $\int_{t_0}^T (b_s^{i,j})^2 ds < \infty$ a.s. □

Lemma 13.1 *Consider a one dimensional Brownian motion and a non-necessary uniform time discretization $t_k = k\frac{T-t_0}{2^n}$ of the interval $[t_0, T]$. Then we have,*

$$(1).\ \lim_{n\to\infty} \sum_{k=0}^{2^n-1} (\Delta t_k)^2 = \lim_{n\to\infty} \sum_{k=0}^{2^n-1} \Delta t_k \Delta W_{t_k} = \lim_{n\to\infty} \sum_{k=0}^{2^n-1} \Delta W_{t_k} \Delta t_k = 0.$$

$$(2).\ \lim_{n\to\infty} \sum_{k=0}^{2^n-1} (\Delta W_{t_k})^2 = \int_{t_0}^T ds = (T - t_0). \qquad (\textit{Convergence in } L^2)$$

where $\Delta t_k = t_{k+1} - t_k$ and $\Delta W_{t_k} = W_{t_{k+1}} - W_{t_k}$. □

Proof The proof for (1). follows from the construction bellow:

$$\lim_{n\to\infty} \sum_{k=0}^{2^n-1} (\Delta t_k)^2 \le \lim_{n\to\infty} \max_k(\Delta t_k) \sum_{k=0}^{2^n-1} \Delta t_k = \lim_{n\to\infty} \max_k(\Delta t_k) \int_{t_0}^T dt = 0$$

For the term (2). with the Brownian motion, we have

$$0 = \lim_{n\to\infty} \min_k(\Delta t_k) \int_{t_0}^T dW_s \le \lim_{n\to\infty} \sum_{k=0}^{2^n-1} \Delta t_k \Delta W_{t_k} \le \lim_{n\to\infty} \max_k(\Delta t_k) \int_{t_0}^T dW_s = 0 = 0.$$

Since ΔW_{t_k} are i.i.d and normally distributed with mean zero and variance Δt_k and by using the strong law of large numbers the following convergence in L^2 is true:

$$\lim_{n\to\infty} \sum_{k=0}^{2^n-1} (\Delta W_{t_k})^2 = \left(\lim_{n\to\infty} \sum_{k=0}^{2^n-1} \Delta t_k \right) = \int_{t_0}^T ds = (T - t_0).$$

Lemma 13.2 *Let us consider the functional $f : [t_0, T] \times I\!R^d \to I\!R$ with continuous partial derivatives $\frac{\partial f}{\partial t}$, $\frac{\partial f}{\partial x^i}$ and $\frac{\partial^2 f}{\partial x^i \partial x^j}$ for $i = 1, \ldots, d$ and a one dimensional Itô Process $(X_t)_{t\in\mathbb{T}}$. For any time discretization $t_k = k\frac{T-t_0}{2^n}$ of the interval $[t_0, T]$. then we have,*

$$(1).\ \lim_{n\to\infty}\sum_{k=0}^{2^n-1}\frac{\partial f}{\partial t}\Delta t_k=\int_{t_0}^{t}\frac{\partial f}{\partial t}ds$$

$$(2).\ \lim_{n\to\infty}\sum_{k=0}^{2^n-1}\frac{\partial f}{\partial x}\Delta X_{t_k}=\int_{t_0}^{t}\frac{\partial f}{\partial x}dX_s=\int_{t_0}^{t}\frac{\partial f}{\partial x}a_s ds+\int_{t_0}^{t}\frac{\partial f}{\partial x}b_s dW_s.$$

$$(3).\ \lim_{n\to\infty}\sum_{k=0}^{2^n-1}\frac{\partial^2 f}{\partial t^2}(\Delta t_k)^2=0\cdot\int_{t_0}^{t}\frac{\partial^2 f}{\partial t^2}ds=0.$$

$$(4).\ \lim_{n\to\infty}\sum_{k=0}^{2^n-1}\frac{\partial^2 f}{\partial x^2}(\Delta X_{t_k})^2=\int_{t_0}^{t}\frac{\partial^2 f}{\partial x^2}b_s^2 ds.$$

where $\Delta t_k=t_{k+1}-t_k$ *and* $\Delta X_{t_k}=X_{t_{k+1}}-X_{t_k}$. □

Proof The result (1). is trivial. The proof for (2).

$$\lim_{n\to\infty}\sum_{k=0}^{2^n-1}\frac{\partial f}{\partial x}\Delta X_{t_k}=\int_{t_0}^{t}\frac{\partial f}{\partial x}dX_s=\int_{t_0}^{t}\frac{\partial f}{\partial x}(a_s ds+b_s dW_s)=\int_{t_0}^{t}\frac{\partial f}{\partial x}a_s ds+\int_{t_0}^{t}\frac{\partial f}{\partial x}b_s dW_s.$$

The proof for (3). consider a uniform time discretization Δt of the interval $[t_0, T]$, then we have

$$\lim_{n\to\infty}\sum_{k=0}^{2^n-1}\frac{\partial^2 f}{\partial t^2}(\Delta t_k)^2=\lim_{n\to\infty}\underbrace{(\Delta t)}_{\to 0}\cdot\underbrace{\int_{t_0}^{t}\frac{\partial^2 f}{\partial t^2}ds}_{bounded}=0$$

The proof for (4).

$$\begin{aligned}\lim_{n\longrightarrow\infty}\sum_{k=0}^{2^n-1}\frac{\partial^2 f}{\partial x^2}(\Delta X_{t_k})^2&=\lim_{n\longrightarrow\infty}\sum_{k=0}^{2^n-1}\frac{\partial^2 f}{\partial x^2}b_{t_k}^2\Delta W_{t_k}^2\\&+\lim_{n\longrightarrow\infty}\underbrace{\sum_{k=0}^{2^n-1}\frac{\partial^2 f}{\partial x^2}a_{t_k}^2\Delta {t_k}^2}_{\longrightarrow 0\ (lemma\ 3.1)}\\&+\lim_{n\longrightarrow\infty}\underbrace{2\sum_{k=0}^{2^n-1}\frac{\partial^2 f}{\partial x^2}a_{t_k}b_{t_k}^2\Delta t_k\Delta W_{t_k}}_{\longrightarrow 0}\quad\left(\text{applying Itôisometry in}\quad L^2\right)\\&=\int_{t_0}^{t}\frac{\partial^2 f}{\partial x^2}b_s^2 ds.\qquad\left(\text{in}\quad L^2\right)\end{aligned}$$

Lemma 13.3 *Under the assumption of the lemmas above, the one dimensional case $d = m = 1$ of the Itô-Formula is given as*

$$f(t, X_t) = f(t_0, X_{t_0}) + \int_{t_0}^{t} \left\{ \frac{\partial f}{\partial s}(s, X_s) + a_s \frac{\partial f}{\partial x}(s, X_s) + \frac{1}{2} b_s^2 \frac{\partial^2 f}{\partial x^2}(s, X_s) \right\} ds \tag{13.5}$$
$$+ \int_{t_0}^{t} b_s \frac{\partial f}{\partial x}(s, X_s) dW_s.$$

Proof For a given discretization of the time interval $[t_0, T]$ by $t_k = k\frac{(T-t_0)}{2^n}$, define $\Delta t_k = t_{k+1} - t_k$; $\Delta X_{t_k} = X_{t_{k+1}} - X_{t_k}$ and $\Delta W_{t_k} = W_{t_{k+1}} - W_{t_k}$. By using the Taylor expansion of order two, we get

$$f(t, X_t) = f(t_0, X_{t_0}) + \sum_{k=0}^{2^n-1} \Delta f(t_k, X_{t_k})$$
$$= f(t_0, X_{t_0}) + \sum_{k=0}^{2^n-1} \frac{\partial f}{\partial t} \Delta t_k + \sum_{k=0}^{2^n-1} \frac{\partial f}{\partial x} \Delta X_{t_k} + \frac{1}{2} \sum_{k=0}^{2^n-1} \frac{\partial^2 f}{\partial x^2} (\Delta X_{t_k})^2 \tag{13.6}$$
$$+ \sum_{k=0}^{2^n-1} \frac{\partial^2 f}{\partial t \partial x} \Delta t_k \Delta X_{t_k} + \frac{1}{2} \sum_{k=0}^{2^n-1} \frac{\partial^2 f}{\partial t^2} (\Delta t_k)^2 + \sum_{k=0}^{2^n-1} R_k. \tag{13.7}$$

where R_k consists of sums of higher order partial derivatives of f as a factor of $(\Delta t)^2$, $\Delta W_{t_k}(\Delta t)^2$, $(\Delta W_{t_k})^2 \Delta t$ and $\Delta W_{t_k} \Delta t$. Using the results of Lemma 13.1, we conclude that $R_k = O\left((\Delta t)^2\right)$ and therefore the remainder term vanish in L^2. Also using the results of Lemma 13.1, all terms with $(\Delta t)^2$ vanish (at least in L^2 if the increment of the Brownian motion appears.) Similar construction could be done for the mixed partial derivatives, which are in general factors either of $(\Delta t)^2$ or $\Delta W_{t_k} \Delta t$. Thus, all terms in (13.7) vanish in L^2:

$$\lim_{n \longrightarrow \infty} \left(\sum_{k=0}^{2^n-1} \frac{\partial^2 f}{\partial t \partial x} \Delta t_k \Delta X_{t_k} + \frac{1}{2} \sum_{k=0}^{2^n-1} \frac{\partial^2 f}{\partial t^2} (\Delta t_k)^2 + \sum_{k=0}^{2^n-1} R_k \right) = 0.$$

The passage to the limit in (13.6), leads to

$$f(t, X_t) = f(t_0, X_{t_0}) + \lim_{n \longrightarrow \infty} \left(\sum_{k=0}^{2^n-1} \frac{\partial f}{\partial t} \Delta t_k + \sum_{k=0}^{2^n-1} \frac{\partial f}{\partial x} \Delta X_{t_k} + \frac{1}{2} \sum_{k=0}^{2^n-1} \frac{\partial^2 f}{\partial x^2} (\Delta X_{t_k})^2 \right).$$

Since $dX_t = a_t dt + b_t dW_t$ and using the results of Lemma 13.2, the one dimensional Itô formula is proved.

Example For $f(t,x) = \frac{1}{2}x^2$ with $X_t = W_t$ and $a_t = 0, b_t = 1$. By applying Itôs formula, we have:

$$\begin{aligned} df &= \frac{\partial f}{\partial t}dt + a_t\frac{\partial f}{\partial x}dt + b_t\frac{\partial f}{\partial x}dW + \frac{1}{2}b_t^2\frac{\partial^2 f}{\partial x^2}dt \\ &= \frac{\partial f}{\partial t}dt + (1)\frac{\partial f}{\partial x}dW + \frac{1}{2}(1)^2\frac{\partial^2 f}{\partial x^2}dt \\ &= \frac{\partial f}{\partial t}dt + \frac{\partial f}{\partial x}dW + \frac{1}{2}\frac{\partial^2 f}{\partial x^2}dt \\ &= \frac{\partial f}{\partial x}dW + \frac{1}{2}\frac{\partial^2 f}{\partial x^2}dt \end{aligned}$$

Hence,

$$\frac{1}{2}dW_t^2 = W_t dW_t + \frac{1}{2}dt$$

and

$$\frac{1}{2}\int dW_s^2 = \int W_s dW_s + \frac{1}{2}\int dt$$

Thus,

$$I_t = \int_0^t W_s dW_s = \frac{1}{2}(W_t^2 - t), \tag{13.8}$$

Note that W_t^2, represents the square of the end value of the Brownian motion. Thus, I_t will be considered as a time process if we change the upper bound of the integration interval. □

Example For $n > 1$; $f(t,x) = x^{n+1}$. By applying Itôs formula for $X_t = W_t$, we have:

$$d(W_t^{n+1}) = (n+1)W_t^n dW_t + \frac{n(n+1)}{2}W_t^{n-1}dt$$

Hence,

$$\int_0^t dW_s^n = \frac{1}{n+1}W_t^{n+1} - \frac{n}{2}\int_0^t W_s^{n-1}ds$$

It is important to note that the integral of a Brownian motion path with respect to time, represented for by $I(W_t) = \int_0^t W_s ds$ is not a stochastic integral. It represents the Area under Brownian motion path, $I(W_t)$ is a normal random variable with mean 0 and variance $\frac{t^3}{3}$: i.e $I(W_t) \sim N(0, \frac{t^3}{3})$. (The proof is similar to the constructions done in Lemma 13.1.) □

Theorem 13.1 *Let us consider the functional* $f : [t_0, T] \times I\!R^d \to I\!R$ *with continuous partial derivatives* $\frac{\partial f}{\partial t}$, $\frac{\partial f}{\partial x^i}$ *and* $\frac{\partial^2 f}{\partial x^i \partial x^j}$ *for* $i = 1, \ldots, d$. *Moreover, consider a* d*-dimensional Itô-Process* $(X_t)_{t\in\mathbb{T}}$, *then we have,*

$$f(t, X_t^1, \ldots, X_t^d) = f(t_0, X_{t_0}^1, \ldots, X_{t_0}^d) + \int_{t_0}^t \frac{\partial f}{\partial s}(s, X_s^1, \ldots, X_s^d)ds \tag{13.9}$$
$$+ \sum_{i=1}^d \int_{t_0}^t \frac{\partial f}{\partial x^i}(s, X_s^1, \ldots, X_s^d)dX_s^i$$
$$+ \frac{1}{2}\sum_{i,j=1}^d \int_{t_0}^t \frac{\partial^2 f}{\partial x^i x^j}(s, X_s^1, \ldots, X_s^d)d < X^i, X^j >_s,$$

where

$$dX_t^i = a^i(s, X_s)ds + \sum_{j=1}^m b^{i,j}(s, X_s)dW_s^j \quad \text{and}$$
$$d < X^i, X^j >_s = \sum_{k=1}^m b^{i,k}(s, X_s)b^{j,k}(s, X_s)ds.$$

where $dW_i dW_j = \delta_{ij}dt$, $dW_i dt = dt dW_i = dt dt = 0$. □

Proof Similar to the one-dimensional case, only with even more complexity.

Theorem 13.2 (Partial integration) *Let us consider two one-dimensional Itô processes* $(X_t)_{t\in\mathbb{T}}$ *and* $(Y_t)_{t\in\mathbb{T}}$ *defined on the same probability space*

$$X_t = X_0 + \int_0^t a_s^1 ds + \int_0^t b_s^1 dW_s, \qquad Y_t = Y_0 + \int_0^t a_s^2 ds + \int_0^t b_s^2 dW_s.$$

The stochastic partial integration formula is given by

$$X_t Y_t = X_0 Y_0 + \int_0^t X_s dY_s + \int_0^t Y_s dX_s + \int_0^t b_s^1 b_s^2 ds. \tag{13.10}$$

Proof See [19].

Example For $X_t = Y_t = W_t$ and $a_t = 0, b_t = 1$. By applying the stochastic partial integration, we get $d(W_t W_t) = W_s dW_s + W_s dW_s + (1)(1)ds$, which is equivalent to $d(W_t^2) = 2W_s dW_s + ds$ and by integrating both sides with respect to the time, it yields $W_t^2 = 2\int_0^t W_s dW_s + \int_0^t 1ds$. Finally, it results $\int_0^t W_s dW_s = \frac{1}{2}(W_t^2 - t)$. □

Remark 13.1 In this remark, we call the attention of the reader to the behavior of time-integral and time-differential of a Brownian motion. Since this is nowhere

differentiable, we use it for the time derivative in the distributional sense of their paths. Thus, we get in both cases a Gaussian stochastic processes. Explicitly, consider a finite difference approximation of ξ_t using a time interval of width Δt, $\xi_{\Delta t}(t) := \frac{W_{t+\Delta t} - W_t}{\Delta t}$ and consider the time integral $Z_t := \int_0^t W_s ds$, representing the area under the path of the Brownian motion $\{W_s\}_{0 \le s \le t}$. □

13.3.2 Multi-indices for Stochastic Integration

In order to be able to define the multiple stochastic integrals, we introduce the following set of multi-indices. Let us consider $m \in \mathbb{N}$ and $F = \{0, 1, \ldots, m\}$. A multi-index α refers to a row vector with components in F such as $\alpha = (j_1, \ldots, j_l)$ where $j_i \in F$, for $1 \le i \le l$.

We denotes the size of α by $l(\alpha) := l$ and by $n(\alpha)$ the number of zero components of α. The set of all multi-indices with respect to F is represented by

$$\mathcal{M} = \bigcup_{l=1}^{\infty} F^l \cup \{v\}, \tag{13.11}$$

where v refers to the empty multi-index with size zero. The following example gives more sense for the definition above:

Example For $\alpha = (1, 0, 2)$ it holds $(\alpha) = 3$ and $n(\alpha) = 1$ and for $\alpha = (1, 0, 0, 2, 3, 1, 0, 0)$ we have $l(\alpha) = 8$and $n(\alpha) = 4$. □

Actually, for $l, k \in \mathbb{N}$, we define the following operations on the multi-index set:

Definition 13.2 ("$-$" *operator*). For $\alpha \in \mathcal{M}$ with $\alpha = (j_1, j_2, \ldots, j_l)$. For $l \ge 1$, we define $\alpha-$ and $-\alpha$ as follow:

$$\alpha- := (j_1, j_2, \ldots, j_{l-1}) \quad \text{and} \quad -\alpha := (j_2, \ldots, j_l).$$

If $l(\alpha) = l > 1$ then, it implies $l(-\alpha) = l(\alpha-) = l - 1$. If $l(\alpha) = l = 1$ then, it implies $-\alpha = \alpha- = v$ and $l(-\alpha) = l(\alpha-) = 0$.

Definition 13.3 ($\star$ *operator*). Let us consider $\alpha = (j_1, j_2, \ldots, j_l)$, $\beta = (i_1, i_2, \ldots, i_k) \in \mathcal{M}$. The operator $\star$ is defined as:

$$\alpha * \beta := (j_1, j_2, \ldots, j_l, i_1, i_2, \ldots, i_k) \quad \text{and} \quad \beta * \alpha := (i_1, i_2, \ldots, i_k, j_1, j_2, \ldots, j_l).$$

Definition 13.4 ("-[i]" *operator*). For $\alpha = (j_1, j_2, \ldots, j_l)$ and $i \in \mathbb{N}$, the Operation "$-[i]$" represents the "i"-times application of "$-$", where the last i components should be deleted:

$$\alpha - [i] := \begin{cases} (j_1, j_2, \ldots, j_{l-i}), & \text{if } i < l; \\ v, & \text{if } i \geq l. \end{cases}$$

It yields $\alpha - [i] - [j] = \alpha - [i + j]$ for $i, j \in \mathbb{N}$. □

Example If $\alpha = (1, 0, 2)$, $\beta = (0, 3, 1)$, then we have

1. $-\alpha = (0, 2)$ and $\alpha - = (1, 0)$,
2. $\alpha \star \beta = (1, 0, 2, 0, 3, 1)$ and $\beta \star \alpha = (0, 3, 1, 1, 0, 2)$,
3. $\alpha - [1] = (1, 0), \alpha - [1] - [1] = \alpha - [2] = (1)$ and $(1, 0, 2) - [i] = v, \forall i \geq 3$.

□

13.3.3 Stochastic Multiple Itô-Integrals

Throughout the following section, all stochastic processes are defined on a probability space $(\Omega, \mathfrak{A}, P)$ with right continuous augmented filtration $\mathfrak{F} = (\mathfrak{F}_t)_{t \in \mathbb{T}}$.

Definition 13.5 Define the set H as a set of stochastic processes $(f_t)_{t \geq 0}$, which are progressively adapted to the associated filtration $\{\mathfrak{F}_t\}_{t \geq 0})$, right continuous and the left limit exists. Conceptively define the sets H_v, $H_{(0)}$, $H_{(1)}$ as follow

1. $H_v := \{f \in H : \forall\, t \geq t_0 \quad |f(t, w)| < \infty \quad \text{a.s.}\}$,
2. $H_{(0)} := \left\{ f \in H : \forall\, t \geq t_0 \quad \int_{t_0}^{t} |f(s, w)| ds < \infty \quad \text{a.s.} \right\}$,
3. $H_{(1)} := \left\{ f \in H : \forall\, t \geq t_0 \quad \int_{t_0}^{t} |f(s, w)|^2 ds < \infty \quad \text{a.s.} \right\}$.

For $j \in F \setminus \{0\}$ one sets $H_{(j)} = H_{(1)}$. □

Definition 13.6 Let us consider $\alpha = (j_1, j_2, \ldots, j_l)$ a multi-index and $(W_t)_{t \geq 0}$ an m-dimensional Brownian motion. For $f \in H_{(\alpha)}$, multiple Itô-Integrals are defined per recursion as follows: □

$$I_\alpha[f(.)]_{t_0,t} := \begin{cases} f(t), & \text{if } l = 0 \\ \int_{t_0}^{t} I_{\alpha-}[f(.)]_{t_0,s} ds, & \text{if } l \geq 1 \text{ and } j_l = 0 \\ \int_{t_0}^{t} I_{\alpha-}[f(.)]_{t_0,s} dW_s^{j_l}, & \text{if } l \geq 1 \text{ and } j_l \geq 1. \end{cases}$$

here $H_{(\alpha)}$ is defined per recursion as

$$H_{(\alpha)} := \{f \in H : \quad I_{(\alpha-)}[f(.)]_{t_0,.} \in H_{(j_l)}\}, \tag{13.12}$$

for $j_l = 0, 1, \ldots, m$ and $l \geq 2$.

Example

$$I_{(1,2)}[f(.)]_{t_0,t} = \int_{t_0}^{t}\int_{t_0}^{s} f(z)dW_z^1 dW_s^2,$$
$$I_{(1,2,0)}[f(.)]_{t_0,t} = \int_{t_0}^{t} I_{(1,2)}[f(.)]_{0,s}ds = \int_{t_0}^{t}\int_{t_0}^{s}\int_{t_0}^{s_1} f(s_2)dW_{s_2}^1 dW_{s_1}^2 ds.$$

□

For simplification, we will use the following notation $I_{\alpha,t} = I_\alpha[1]_{0,t}$ and $W_t^0 = t$. Moreover, we will use the Kronecker symbol δ for $j_{i_1}, j_{i_2} = 0, 1, \ldots, l.$ defined by $\delta_{j_{i_1}, j_{i_2}} = 1$ if $j_{i_1} = j_{i_2}$ and 0 else.

Theorem 13.3 *Let us consider $l \in \mathbb{N}$ and $\alpha = (j_1, ..., j_l) \in \mathcal{M}$. For $t \geq 0$, we have*

$$I_{(j),t} I_{(\alpha),t} = \sum_{i=0}^{l} I_{(\alpha-[l-i])*(j,j_{i+1},...,j_l),t} + \sum_{i=1}^{l} B_{jj_i} I_{(\alpha-[l-i+1])*(0,j_{i+1},...,j_l),t}, \quad (13.13)$$

where $B_{jj_i} = \delta_{j,j_i}(1 - \delta_{0,j})$. □

Proof By using partial integration, we get:

$$\begin{aligned} d(I_{(j),t} I_{\alpha,t}) &= I_{(j),t} d(I_{\alpha,t}) + I_{\alpha,t} d(I_{(j),t}) + (1 - \delta_{0,j}) I_{\alpha-} dW_t^j dW_t^{j_l} \\ &= I_{(j),t} d(I_{\alpha,t}) + I_{\alpha,t} d(I_{(j),t}) + (1 - \delta_{0,j})\delta_{jj_l} I_{\alpha-,t} dt \\ &= I_{(j),t} d(I_{\alpha,t}) + I_{\alpha,t} d(I_{(j),t)}) + B_{jj_l} I_{\alpha-,t} dt \\ &= I_{(j),t)} I_{\alpha-,t} dW_t^{j_l} + I_{\alpha,t} d(I_{(j),t}) + B_{jj_l} I_{\alpha-,t} dt. \end{aligned}$$

For simplification, let us define the terms $A_{\alpha,t}^j = I_{(j),t} I_{\alpha,t}$ for $\alpha \in \mathcal{M}$, we obtain

$$\begin{aligned} A_{\alpha,t}^j &= \int_0^t I_{\alpha,s} d I_{(j),s} + \int_0^t I_{(j),s} I_{\alpha-,s} dW_s^{j_l} + B_{jj_l} \int_0^t I_{\alpha-,s} ds \\ &= \int_0^t I_{\alpha,s} dW_s^j + \int_0^t A_{(\alpha-[1]),s}^j dW_s^j + B_{jj_l} I_{(\alpha-[1])*(0),t}, \\ &= I_{\alpha*(j),t} + \int_0^t A_{(\alpha-[1]),s}^j dW_s^j + B_{jj_l} I_{(\alpha-[1])*(0),t}. \end{aligned}$$

Per induction over l in α in $A_{\alpha-[1],t}^j$

$$\begin{aligned} A_{\alpha,t}^j &= I_{\alpha*(j),t} + \int_0^t I_{(\alpha-[1])*(j),s_l} dW_{s_l}^{j_l} + \int_0^t \int_0^{s_l} A_{(\alpha-[2]),s_{l-1}}^j dW_{s_{l-1}}^{j_{l-1}} dW_{s_l}^{j_l} \\ &\quad + B_{jj_{l-1}} \int_0^t I_{\alpha-[2]*(0),t} dW_{s_l}^{j_l} + B_{jj_l} I_{(\alpha-[1])*(0),t} \\ &= I_{\alpha*(j),t} + I_{(\alpha-[1])*(j,j_l),t} + \int_0^t \int_0^{s_l} A_{(\alpha-[2]),s_{l-1}^j} dW_{s_{l-1}}^{j_{l-1}} dW_{s_l}^{j_l} \\ &\quad + B_{jj_{l-1}} I_{(\alpha-[2])*(0,j_l),t} + B_{jj_l} I_{(\alpha-[1])*(0),t} \end{aligned}$$

Now the same procedure will be applied to $A_{(\alpha-[2]),s_{l-1}^j}$, we get:

$$A_{\alpha,t}^j = \sum_{i=1}^{l} I_{(\alpha-[l-i])*(j,j_{i+1},\cdots,j_l),t} + \int_0^t \int_0^{s_l} \cdots \int_0^{s_2} A_{(\alpha-[l]),s_1}^j dW_{s_1}^{j_1} \cdots dW_{s_l}^{j_l} + \sum_{i=1}^{l} B_{jj_l} I_{(\alpha-[l-i+1])*(0,j_{i+1},\cdots,j_l),t}.$$

Note that

$$A_{(\alpha-[l]),s_1}^j = I_{(j),s_1} I_{(\alpha-[l]),j_l} = I_{(j),s_1} I_{v,s_1} = I_{(j),s_l} = \int_0^{s_1} dW_s^j, \tag{13.14}$$

hence, we have

$$\begin{aligned} I_{(\alpha-[l])*(j,j_1,\cdots,j_l),t} &= \int_0^t \int_0^{s_l} \cdots \int_0^{s_2} A_{(\alpha-[l]),s_1}^j dW_{s_1}^{j_1} \cdots dW_l^{j_l} \\ &= \int_0^t \int_0^{s_l} \cdots \int_0^{s_2} \int_0^{s_1} dW_s^j dW_{s_1}^{j_1} \cdots dW_l^{j_l}. \end{aligned} \tag{13.15}$$

by replacing (13.14) and (13.15) in (13.14), we obtain (13.13). Thus, we achieve the proof of the theorem.

The following corollary gives a clear idea about an interesting class of multiple stochastic integrals

Corollary 13.1 *Consider $l, j \in \mathbb{N}$ and $\alpha = (j, j, \ldots, j)$ with $l(\alpha) = l$. It holds:*

$$I_{\alpha,t} = \begin{cases} \frac{t^l}{l!} & \text{for } j = 0, \\ \frac{1}{l}(W_t^j I_{\alpha-,t} - t I_{\alpha-[2],t}) & \text{for } j \geq 1. \end{cases}$$

Proof From Theorem 13.3 ($B_{0,0} = 0$) it follows

$$\begin{aligned} t I_{\alpha,t} = I_{(0),t} I_{\alpha,t} &= \sum_{i=0}^{l} I_{(\alpha-[l-i])*(j,j_{i+1},\cdots,j_l)} \\ &= \sum_{i=0}^{l} I_{\underbrace{(0,0,\ldots,0)}_{(l+1)-times}} \\ &= (l+1)\frac{t^{l+1}}{(l+1)!}. \end{aligned} \tag{13.16}$$

The length of the multi-index $((\alpha - [l-i]) * (j, j_{i+1}, \cdots, j_l))$ is determined by:

$$\begin{aligned} l((\alpha - [l-i]) * (j, j_{i+1}, \cdots, j_l)) &= l(\alpha - [l-i]) + l((j, j_{i+1}, \cdots, j_l)) \\ &= l(\alpha - [l-i]) + l((j)) + l(j_{i+1}, \cdots, j_l)) \\ &= l - (l-i) + 1 + (l-i) \\ &= l + 1. \end{aligned}$$

From (13.16), we get $I_{\alpha,t} = \frac{t^l}{l!}$. For $j \geq 1$ it yields $B_{jj} = 1$. Moreover,

$$\begin{aligned} I_{(j),t} I_{\alpha-,t} &= \sum_{i=0}^{l-1} I_{\underbrace{(j, \ldots, j)}_{l-times}} + \sum_{i=1}^{l-1} I_{((\alpha)-[1]-[l-i+1])*(0, j_{i+1}, \cdots, j_l)} \\ &= l I_{\underbrace{(j, \ldots, j)}_{l-times}} + \sum_{i=1}^{l-1} I_{\underbrace{((\alpha) - [1] - [l-i+1]) * (0, j, \cdots, j)}_{size=(l-1)}} \\ &= l I_{\underbrace{(j, \ldots, j)}_{l-times}} + \sum_{i=1}^{l-1} I_{\underbrace{((\alpha) - [2] - [l-i]) * (0, j, \cdots, j)}_{size=(l-1)}}. \end{aligned} \tag{13.17}$$

Using Theorem 13.3 for $j = 0$, it follows

$$I_{(0),t} I_{\alpha-[2],t} = t I_{\alpha-[2],t} = \sum_{i=1}^{l-1} I_{\underbrace{((\alpha) - [2] - [l-i]) * (0, j, \cdots, j)}_{size=(l-1)}}. \tag{13.18}$$

From (13.17) and (13.18) it follows: $I_{(j),t} I_{\alpha-,t} = l I_{\underbrace{(j, \ldots, j)}_{(l)-times}} + t I_{\alpha-[2],t}$. Thus

$$I_{\underbrace{(j, \ldots, j)}_{l-times}} = \frac{1}{l} (I_{(j),t} I_{\alpha-,t} - t I_{\alpha-[2],t})$$

Lemma 13.4 *We have the following values of the multiple stochastic integrals for the special case $\alpha = (j, j, \ldots, j) \in \mathcal{M}$:*

$$I_{(j,j,j),t} = \frac{1}{3}\Big(I_{(j),t} \frac{1}{2}(I^2_{(j),t} - t) - t I_{(j),t}\Big) = \frac{1}{3!}\Big(I^3_{(j),t} - 3t I_{(j),t}\Big), \tag{13.19}$$

$$I_{(j,j,j,j),t} = \frac{1}{4!}\Big(I^4_{(j),t} - 6t I^2_{(j),t} + 3t^2\Big), \tag{13.20}$$

$$I_{(j,j,j,j,j),t} = \frac{1}{5!}\Big(I^5_{(j),t} - 10t I^3_{(j),t} + 15t^2 I_{(j),t}\Big), \tag{13.21}$$

$$I_{(j,j,j,j,j,j),t} = \frac{1}{6!}\Big(I^6_{(j),t} - 15t I^4_{(j),t} + 45t^2 I^2_{(j),t} - 15t^3\Big), \tag{13.22}$$

$$I_{(j,j,j,j,j,j,j),t} = \frac{1}{7!}\Big(I^7_{(j),t} - 21tI^5_{(j),t} + 105t^2 I^3_{(j),t} - 105t^3 I_{(j),t}\Big). \tag{13.23}$$

□

Proof Note that, since $(j, j) - [2] = v$, we have

$$I_{(j,j),t} = \frac{1}{2}(I^2_{(j),t} - t) = \frac{1}{2}\Big((W^j_t)^2 - t\Big). \tag{13.24}$$

The proof of the other multiple integrals is left to the reader (use Corollary 13.1).

To approximate numerical solutions for the SDE (13.3) we consider a generalized Milstein method. The starting point for development of the Milstein method is the stochastic Itô-Taylor expansion, compare [20–22, 26]. Thus, for a given functional $f : [t_0, T] \times I\!R^d \to I\!R$ with all its derivatives are smooth functions, the associated Itô-Taylor expansion is given by

$$f(\tau, \mathbf{X}_\tau) = \sum_{\alpha \in \mathcal{A}_\gamma} \mathbf{I}_\alpha \left[f_\alpha(\rho, \mathbf{X}_\rho)\right]_{\rho,\tau} + \sum_{\alpha \in \mathcal{B}_\gamma} \mathbf{I}_\alpha \left[f_\alpha(\cdot, \mathbf{X}_\cdot)\right]_{\rho,\tau}, \tag{13.25}$$

where ρ and τ are two stop times processes, α a multi-index in the set of all multi-indices $\mathcal{M}$, A_γ a hierarchical set and B_γ its remainder set defined as

$$\begin{aligned} \mathcal{A}_\gamma &= \Big\{\alpha \in \mathcal{M} : \quad l(\alpha) + n(\alpha) \le 2\gamma \quad \text{or} \quad l(\alpha) = n(\alpha) = \gamma + \frac{1}{2}\Big\}, \\ \mathcal{B}_\gamma &= \Big\{\alpha \in \mathcal{M}\backslash\mathcal{A}_\gamma : \quad -\alpha \in \mathcal{A}_\gamma\Big\}, \end{aligned} \tag{13.26}$$

with $l(\alpha)$ and $n(\alpha)$ refer respectively, to the length and the number of zeros of the multi-index α, and $-\alpha$ is the multi-index α without the first component. Note that for each construction of the sets A_γ and B_γ in (13.26), γ is allowed to take the values $\gamma = 0.5, 1, 1.5, 2, \ldots$. For example, in a two-dimensional case, the corresponding hierarchical set $\mathcal{A}_1$ and its remainder set $\mathcal{B}_1$ are

$$\begin{aligned} \mathcal{A}_1 &= \Big\{v, (0), (1), (2), (1, 1), (1, 2), (2, 2), (2, 1)\Big\}, \\ \mathcal{B}_1 &= \Big\{(0, 0), (0, 1), (0, 2), (1, 0), (2, 0), (0, 1, 1), (0, 1, 2), (1, 2, 2), (0, 2, 2), \\ &\qquad (0, 2, 1), (1, 1, 1), (1, 1, 2), (1, 2, 1), (2, 1, 1), (2, 1, 2), (2, 2, 2), (2, 2, 1)\Big\}. \end{aligned}$$

where v is the so-called empty index, see [20–22, 26, 28] among others. In the Itô expansion (13.25), $\mathbf{I}_\alpha\left[f_\alpha(\rho, \mathbf{X}_\rho)\right]$ with $\alpha = (j_1, j_2, \ldots, j_l)$, denotes the multiple Itô integrals of the function f and it is defined by

$$\mathbf{I}_{\alpha}[f(\cdot,\mathbf{X}_{\cdot})]_{t_0,t}=\begin{cases} f(t,\mathbf{X}_t), & \text{if} \quad l=0,\\ \displaystyle\int_{t_0}^{t}\mathbf{I}_{\alpha-}[f(\cdot,\mathbf{X}_{\cdot})]_{t_0,s}ds, & \text{if} \quad l\geq 1 \quad \text{and} \quad j_l=0,\\ \displaystyle\int_{t_0}^{t}\mathbf{I}_{\alpha-}[f(\cdot,\mathbf{X}_{\cdot})]_{t_0,s}d\mathbf{W}_s^{j_l}, & \text{if} \quad l\geq 1 \quad \text{and} \quad j_l\geq 1, \end{cases} \tag{13.27}$$

where $\alpha-$ is the the multi-index α without the last component. As examples of the multiple Itô integrals (13.27), we consider

$$\begin{aligned}\mathbf{I}_{(1,2)}[f(\cdot)]_{t_0,t}&=\int_{t_0}^{t}\int_{t_0}^{s}f(z)d\mathbf{W}_z^1d\mathbf{W}_s^2,\\ \mathbf{I}_{(1,2,0)}[f(\cdot)]_{t_0,t}&=\int_{t_0}^{t}\mathbf{I}_{(1,2)}[f(.)]_{0,s}ds,\\ &=\int_{t_0}^{t}\int_{t_0}^{s}\int_{t_0}^{s_1}f(s_2)d\mathbf{W}_{s_2}^1d\mathbf{W}_{s_1}^2ds.\end{aligned}$$

For the time discretization, we divide the time interval $[t_0, T]$ into equidistant subintervals $[t_n, t_{n+1}]$ of length Δt such that $t_n = t_0 + n\Delta t$, $n = 0, 1, \ldots$. From the Itô-Taylor expansion (13.25) we construct the discrete approximation

$$f(t_{n+1},\mathbf{Y}_{t_{n+1}})=\underbrace{\sum_{\alpha\in A_\gamma}\mathbf{I}_{\alpha}\left[f_{\alpha}(t_n,\mathbf{Y}_{t_n})\right]_{t_n,t_{n+1}}}_{\text{Main approximation}}+\underbrace{\sum_{\alpha\in\mathcal{B}_\gamma}\mathbf{I}_{\alpha}\left[f_{\alpha}(\cdot,\mathbf{Y}_{\cdot})\right]_{t_n,t_{n+1}}}_{\text{Remainder}}, \tag{13.28}$$

where $\mathbf{Y}_{t_n}$ denotes the approximation of the solution $\mathbf{X}_t$ of the SDE (13.3) at the time $t = t_n$. For independent one-dimensional Wiener processes $(\mathbf{W}_t^{j_1})_{t\geq 0}$ and $(\mathbf{W}_t^{j_2})_{t\geq 0}$, with $j_1 \neq j_2$, the double Itô integrals $\mathbf{I}_{(j_1,j_2)}$ are defined as

$$\mathbf{I}_{(j_1,j_2)t_0,t}=\int_{t_0}^{t}\int_{t_0}^{s_1}d\mathbf{W}_s^{j_1}d\mathbf{W}_{s_1}^{j_2}. \tag{13.29}$$

Since this integral cannot be calculated exactly, a numerical approximation is required, see for instance [20, 22, 26]. Here, we consider the Fourier series expansion

$$\begin{aligned}\mathbf{I}_{(j_1,j_2)}^{p}=&\frac{1}{2}\Delta t\epsilon_{j_1}\epsilon_{j_2}+\Delta t\sqrt{\rho_p}(\mu_{j_1,p}\epsilon_{j_2}-\mu_{j_2,p}\epsilon_{j_1})+\\ &\frac{\Delta t}{2\pi}\sum_{r=1}^{p}\frac{1}{r}(\zeta_{j_1,r}(\sqrt{2}\epsilon_{j_2}+\eta_{j_2,r})-\zeta_{j_2,r}(\sqrt{2}\epsilon_{j_1}+\eta_{j_1,r})),\end{aligned} \tag{13.30}$$

where ϵ_{j_1}, ϵ_{j_2}, $\mu_{j_1,p}$, $\mu_{j_2,p}$, $\zeta_{j_1,r}$, $\zeta_{j_2,r}$, $\eta_{j_2,r}$ and $\eta_{j_1,r}$ are random variables pairwise independent $\mathcal{N}(0, 1)$, and ρ_p is a constant defined as

$$\rho_p = \frac{1}{2\pi^2} \sum_{r=p+1}^{\infty} \frac{1}{r^2}.$$

In (13.30), p is the order of the approximation on an interval. Based on a theorem in [26] that establish the relation between the order of a one-step approximation and the order of the scheme generated by such approximation, one can obtain schemes of order p by means of one-step approximations of local order $p+1$. For example, the truncated Itô-Taylor expansion of order p of the Itô process $\mathbf{X}_t$ (i.e., the expression obtained from the Itô-Taylor expansion removing the terms which contain multiple integrals of multiplicities equal to or greater than $p+1$) is an approximation of local order $p+1$ if the coefficients of the equation are continuous, satisfy both Lipschitz and linear growth conditions. The scheme obtained with the truncated Itô-Taylor expansion of order p will be called the order p weak Taylor scheme, see [20–22] for details. Not that the error estimate of the approximation $\mathbf{I}_{(j_1,j_2)^p}$ in (13.30) of the double Itô integral $\mathbf{I}_{(j_1,j_2)}$ is given in second moment by

$$\mathbf{E}\left(\left|\mathbf{I}^p_{(j_1,j_2)} - \mathbf{I}_{(j_1,j_2)}\right|^2\right) = \rho_p(\Delta t)^2, \tag{13.31}$$

where $E(w)$ denotes the expectation of a generic solution w. In the current study, to approximate numerical solutions to the SDE (13.3) a generalized Milstein scheme is implemented based on the Itô-Taylor expansion (13.28) as

$$\mathbf{Y}^k_{n+1} = \mathbf{Y}^k_n + \mathcal{F}^k(t_n, \mathbf{Y}_n)\Delta t + \sum_{j=1}^{N+2} \mathcal{G}^{k,j}(t_n, \mathbf{Y}_n)\Delta \mathbf{W}^j_{t_n} + \sum_{j_1,j_2=1}^{N+2} L^{j_1}\mathcal{G}^{k,j_2}(t_n, \mathbf{Y}_n)\mathbf{I}_{(j_1,j_2)}, \tag{13.32}$$

where $\Delta \mathbf{W}^1_{t_n}, \ldots, \Delta \mathbf{W}^{N+2}_{t_n}$ are independent random Gaussian variables $\mathcal{N}(0, \Delta t)$ and the differential operators L^j are given as

$$L^0 = \frac{\partial}{\partial t} + \sum_{k=1}^{N+2} \mathcal{F}^k_t \frac{\partial}{\partial x^k} + \frac{1}{2}\sum_{k,i=1}^{d}\sum_{j=1}^{N+2} \mathcal{G}^{i,j} b^{k,j} \frac{\partial^2}{\partial x^i \partial x^k},$$

$$L^j = \sum_{i=1}^{N+2} \mathcal{G}^{i,j} \frac{\partial}{\partial x^i}, \qquad j = 1, 2, \ldots, N+2.$$

Note that the first-order Milstein scheme is given by the summation over all multi-index of the hierarchical set A_1. For the computation of the integrals $\mathbf{I}_{(j,j)}$ for $j = 0, 1, \ldots, N+2$, we have used the classical Itô calculus, we refer for example to [20, 22]. Notice that the accuracy of the Itô-Taylor expansion (13.28) depends on the number p such that high accuracy is obtained for large values of p. However,

large values of p can lead to high computational cost and may limit the efficiency of the overall procedure. In the present study, all the simulations are performed with $p = 100$ which is enough to ensure an accurate representation of the Itô-Taylor expansion (13.28).

13.3.4 Itô-Taylor Schemes for Systems Driven by One Noise

Let $(W_t)_{t\in[t_0,T]}$ be an m-dimensional Brownian motion defined on a $(\Omega, \mathcal{A})^m$ with right continuous augmented filtration $\mathcal{F} = (\mathcal{F}_t)_{t\in[0,T]}$. Consider the following $d-$ dimensional Itô process $(X_t^1 \ldots, X_t^d)$, which satisfies the stochastic differential (13.33):

$$X_t^i = X_0^i + \int_0^t a_s^i ds + \sum_{j=1}^{m} \int_0^t b_s^{i,j} dW_s^j \tag{13.33}$$

where for all $i = 1, \ldots, d$, and $j = 1, \ldots, m$; the drift vector $(a_t^i)_{t\in[0,T]}$ and the diffusion matrix $(b_t^{i,j})_{t\in[0,T]}$ are $\mathcal{F}_t$ adapted and satisfy $\int_0^T a_s^i ds < \infty$ and $\int_0^T (b_s^{i,j})^2 ds < \infty$ a.s.

For any partition $0 = t_0 < t_1 < \cdot < t_N = T$ of the time interval $[0, T]$ with step sizes $\Delta t_n = t_{n+1} - t_n$ and maximum step-size $\Delta = \max_n \Delta t_n$, let Y_n^Δ be a numerical approximation of the exact solution X_{t_n}. We have to distinct between the strong and the weak convergence of X_{t_n}. We said that the Y_n is a strong approximation of order γ if it exists $K_{p,T} > 0$ such that

$$E_s^\gamma(Y_n^\Delta) := \left(E|Y_{N_T}^\gamma - X_T|^p\right)^{\frac{1}{p}} \leq K_{p,T}\Delta^\gamma \quad \text{with} \quad \lim_{N_T\to\infty} E_s^\gamma(Y_n^\Delta) = 0. \tag{13.34}$$

and we said that Y_n is a weak approximation of order β if it exists $K_{g,T} > 0$ such that

$$E_w^\beta(Y_n^\Delta) := \left|Eg\left(Y_{N_T}^\beta\right) - Eg(X_T)\right| \leq K_{g,T}\Delta^\beta \quad \text{with} \quad \lim_{N_T\to\infty} E_w^\beta(Y_n^\Delta) = 0, \tag{13.35}$$

where g any polynomial function and p is in general one or two. However, we have to note that all numerical approximation in the stochastic case are results in the mean theory in L^2.

Remark 13.2 In the topic of numerical methods for SPDEs the overall convergence rate represents the scheme dependency to temporal and spatial discretization, which is usually expressed in terms of the computational cost. For the one dimensional case, if N is the number of all operations needed to compute an iteration per time (arithmetical operations, random number and function evaluations) and if the constant M refers the number of time steps $\Delta = \frac{T}{M}$. Suppose that the scheme has the following error bound

$$\sup_{k=0,\ldots,M}\left(\left|\mathbf{v}_{t_k}-\mathbf{u}_k^{(N,M)}\right|^2_{L^2(D)}\right)^{\frac{1}{2}}\leq K_T\left(\frac{1}{N^\alpha+M^\beta}\right) \tag{13.36}$$

where $\mathbf{v}_{t_k}$ is the exact solution at $t=t_k$ and $\mathbf{u}_k^{(N,M)}$ is the corresponding numerical approximation. Thus, for $\alpha,\beta>0$, the optimal overall rate $\gamma=\frac{\alpha\beta}{\alpha+\beta}$ with respect to the computational cost is given by

$$\max_{k=0,\ldots,M}\left(\left|\mathbf{v}_{t_k}-\mathbf{u}_k^{(N,M)}\right|^2_{L^2(D)}\right)\leq K_T\,(NM)^{-\gamma}\,. \tag{13.37}$$

For example if $\alpha=\frac{1}{2}$ and $\beta=1$, then $\gamma=\frac{1}{3}$. For more details we refer to [18]. □

We consider a regular function $f:\mathbb{R}^d\to\mathbb{R}$ and suppose that the assumptions of the existence of the numerical solution given in [20] are satisfied. Thus, the strong Itô-Taylor scheme of order $\gamma=0.5,\ 1,\ 1.5,\ 2,\ldots$ is given by:

$$\begin{aligned}Y_0&=\xi_0,\\ Y_{n+1}&=\sum_{\alpha\in\mathcal{A}_\gamma}I_\alpha[f_\alpha(t_n,Y_n)]_{t_n,t_{n+1}}=Y_n+\sum_{\alpha\in\mathcal{A}_\gamma\setminus\{v\}}I_\alpha[f_\alpha(t_n,Y_n)]_{t_n,t_{n+1}},\end{aligned} \tag{13.38}$$

where I_α represents the multiple Itô-Integrals and $\mathcal{A}_\gamma$ is given by

$$\mathcal{A}_\gamma=\{\alpha\in\mathcal{M}_m|\ \ell(\alpha)+n(\alpha)=2\gamma\text{ or }\ell(\alpha)=n(\alpha)=\gamma+0.5\}\,. \tag{13.39}$$

For the weak approximation we change the the index set $\mathcal{A}_\gamma$ by $\mathcal{A}_\beta$ such that

$$\mathcal{A}_\gamma=\{\alpha\in\mathcal{M}_m|\ \ell(\alpha)\leq\beta\}\,. \tag{13.40}$$

In more detailed form, we rewrite the scheme (13.38):

$$\begin{aligned}Y_0&=\xi_0,\\ Y_{n+1}&=Y_n+I_{(0)}[a(t,Y_n)]_{\Delta t_n}+\sum_{j=1}^m I_{(j)}[b^j(t,Y_n)]_{\Delta t_n} &(13.41)\\ &+\sum_{j=1}^m I_{(j,j)}[L^jb^j(t,Y_n)]_{\Delta t_n} &(13.42)\\ &+\sum_{j=1}^m I_{(j,0)}[L^ja(t,Y_n)]_{\Delta t_n}+\sum_{j=1}^m I_{(0,j)}[L^0b^j(t,Y_n)]_{\Delta t_n} &(13.43)\\ &+\sum_{j=1}^m I_{(0,0)}[L^0a(t,Y_n)]_{\Delta t_n}+\sum_{j=1}^m I_{(j,j,j)}[L^jL^jb^j(t,Y_n)]_{\Delta t_n} &(13.44)\\ &+\sum_{j=1}^m I_{(j,j,0)}[L^jL^ja(t,Y_n)]_{\Delta t_n}+\sum_{j=1}^m I_{(j,0,j)}[L^jL^0b^j(t,Y_n)]_{\Delta t_n} &(13.45)\\ &+\sum_{j=1}^m I_{(0,j,j)}[L^0L^jb^j(t,Y_n)]_{\Delta t_n}+\sum_{j=1}^m I_{(j,j,j,j)}[L^jL^jL^jb^j(t,Y_n)]_{\Delta t_n}, &(13.46)\end{aligned}$$

where Euler Maruyama (13.42), Milstein (13.42)–(13.42), Taylor of order 1.5 represented by (13.42)–(13.44) and Taylor of order 2.0 is represented by the equations (13.42)–(13.46), for $i = 1, \ldots, d$ and $j = 1, \ldots, m$ the differential operators L^j for $j = 0, 1, \ldots, m$ are given by

$$L^0 = \frac{\partial}{\partial t} + \sum_{k=1}^{d} a_t^k \frac{\partial}{\partial x^k} + \frac{1}{2} \sum_{k,i=1}^{d} \sum_{j=1}^{m} b^{i,j} b^{k,j} \frac{\partial^2}{\partial x^i \partial x^k}, \tag{13.47}$$

$$L^j = \sum_{i=1}^{d} b^{i,j} \frac{\partial}{\partial x^i}. \tag{13.48}$$

The Itô-Taylor schemes (13.42)–(13.46) correspond to the following index sets: For $\gamma = 0$ the index set

$$\mathcal{A}_{0.0} = \{v\},$$

represents the initial guess of the numerical scheme. If $\gamma = 0.5$, the construction of the index set

$$\mathcal{A}_{0.5} = \mathcal{A}_{0.0} \cup \Big\{(0), (1)\Big\},$$

leads to the Euler–Maruyama scheme. If $\gamma = 1$ then the index set

$$\mathcal{A}_{1.0} = \mathcal{A}_{0.5} \cup \Big\{(1, 1)\Big\},$$

corresponds to the first order Itô-Taylor scheme (called also Milstein scheme), and if $\gamma = 1.5$ the index-set is

$$\mathcal{A}_{1.5} = \mathcal{A}_{1.0} \cup \Big\{(0, 0), (1, 0), (0, 1), (1, 1, 1)\Big\}.$$

If $\gamma = 2.0$ the index set is

$$\mathcal{A}_{2.0} = \mathcal{A}_{1.5} \cup \Big\{(1, 1, 0), (0, 1, 1), (1, 0, 1), (1, 1, 1, 1)\Big\}.$$

The entries of the Itô-Taylor approximation are the stochastic integrals with index length less than or equal four. These stochastic integrals can be classified in four types. We present their explicit form for autonomous SDE (i.e. autonomous drift and diffusion):

$\ell(\alpha) = 1$, In this case, we define the following deterministic and stochastic integral:

$$I_{(0)}[a(t_n, X_{t_n})]_{\Delta t_n} = a(t_n, X_{t_n}) \Delta t_n. \tag{13.49}$$

$$I_{(1)}[b(t_n, X_{t_n})]_{\Delta t_n} = b(t_n, X_{t_n}) \int_{t_n}^{t_{n+1}} dW_s^1, \tag{13.50}$$

with index $\alpha \in \mathcal{M}_1$ such that $n(\alpha) \leq 1$.

$\ell(\alpha) = 2$, stochastic integral with index $\alpha \in \mathcal{M}_1$ and $\ell(\alpha) = 2$:

$$I_{(1,1)}[L^1 b(t_n, X_{t_n})]_{\Delta t_n} = b(t_n, X_{t_n}) \frac{\partial b}{\partial x}(t_n, X_{t_n}) \int_{t_n}^{t_{n+1}} \int_{t_n}^{t} dW_s^1 dW_t^1 \tag{13.51}$$

$$= b(t_n, X_{t_n}) \frac{\partial b}{\partial x}(t_n, X_{t_n}) I_{(1,1),\Delta t_n},$$

$$I_{(1,0)}[L^1 a(t_n, X_{t_n})]_{\Delta t_n} = b(t_n, X_{t_n}) \frac{\partial a}{\partial x}(t_n, X_n) \int_{t_n}^{t_{n+1}} \int_{t_n}^{t} dW_s^1 dt \tag{13.52}$$

$$= b(t_n, X_{t_n}) \frac{\partial a}{\partial x}(t_n, X_n) I_{(1,0),\Delta t_n},$$

$$I_{(0,1)}[L^0 b(t_n, X_n)]_{\Delta t_n} = \left(a \frac{\partial b}{\partial x} + \frac{1}{2} b^2 \frac{\partial^2 b}{\partial x^2} \right)(t_n, X_{t_n}) \int_{t_n}^{t_{n+1}} \int_{t_n}^{t} ds dW_t \tag{13.53}$$

$$= \left(a \frac{\partial b}{\partial x} + \frac{1}{2} b^2 \frac{\partial^2 b}{\partial x^2} \right)(t_n, X_{t_n}) I_{(0,1),\Delta t_n},$$

$$I_{(0,0)}[L^0 a(t_n, X_n)]_{\Delta t_n} = \left(a \frac{\partial a}{\partial x} + \frac{1}{2} b^2 \frac{\partial^2 a}{\partial x^2} \right)(t_n, X_n) \int_{t_n}^{t_{n+1}} \int_{t_n}^{t} ds dt, \tag{13.54}$$

$\ell(\alpha) = 3$, stochastic integral with index $\alpha \in \mathcal{M}_1$ and $\ell(\alpha) = 3$:

$$I_{(1,1,1)}[L^1 L^1 b(t_n, X_n)]_{\Delta t_n} = \left(b\,(b')^2 + b^2 b'' \right)(t_n, X_n) \int_{t_n}^{t_{n+1}} \int_{t_n}^{t} \int_{t_n}^{s} dW_r dW_s dW_t \tag{13.55}$$

$$= \left(b\,(b')^2 + b^2 b'' \right)(t_n, X_n) I_{(1,1,1),\Delta t_n},$$

$$I_{(1,1,0)}[L^1 L^1 a(t_{,}.X_n)]_{\Delta t_n} = \left(ba' + ba'' \right)(t_n, X_n) I_{(1,1,0),\Delta t_n} \tag{13.56}$$

$$I_{(1,0,1)}[L^1 L^0 b(t_{,}.X_n)]_{\Delta t_n} = \left(ba' b' + abb'' + b^2 b' b'' + \frac{1}{2} b^2 b''' \right)(t_n, X_n) I_{(1,0,1),\Delta t_n}, \tag{13.57}$$

$$I_{(0,1,1)}[L^0 L^1 b(t_{,}.X_n)]_{\Delta t_n} = \left(a(bb')' + \frac{1}{2} a^2 (bb')''' \right)(t_n, X_n) I_{(0,1,1),\Delta t_n}. \tag{13.58}$$

$\ell(\alpha) = 4$, provided that $n(\alpha) = 0$, we define the multiple stochastic integral

$$I_{(1,1,1,1)}[L^1 L^1 L^1 b(t_n, X_n)]_{\Delta t_n} = b \left(b \left(b(bb') \right)' \right)' I_{(1,1,1,1),\Delta t_n}, \tag{13.59}$$

where a', b' represents the spatial derivatives of the drift and the diffusion in the autonomous case. The general case needs the use of the stochastic differential operators L^0 and L^1. The integrals $I_{(1)}, \ldots, I_{(1,1,1,1)}$ are analytically formulated by the exact expressions in [10].

In the present paper, we deal with Dirichlet external boundary conditions and Neuman-like internal boundary conditions. The solutions on the common interfaces of the subdomains are effects caused by a backward step of the solutions on interiors of the subdomains. For the considered boundary-value equations, we assume non-flux boundary conditions (i.e. homogeneous Neumann conditions), which have been widely used to model practical problems from engineering and industrial applications, such as stochastic advection-diffusion equations, stochastic Burgers equation, stochastic Korteweg-de Vries equation, and stochastic Navier-Stokes equations. For more details, we refer to the works [10, 43, 47].

13.4 Numerical SDE and SDES Examples

In this section numerical results are presented for the reduced model of prebiotic evolution depicted in Fig. 13.1. We also illustrate the performance of the Milstein scheme for two problems in SDE with known exact solutions. In all our simulations we perform 10, 000 realizations and mean solutions are displayed. Note that equations with known analytical solutions are used to quantify the errors and to examine the convergence features of the considered method. For the sake of comparison we also consider the canonical Euler–Maruyama method widely used in the literature for solving SDE, compare for instance [20, 22, 43, 44, 46, 47].

13.4.1 A Stochastic Linear Equation

We consider the stochastic Black-Scholes equation used in option pricing [22]

$$dX_t = \lambda X_t dt + \mu X_t dW_t, \qquad X_0 = x_0. \tag{13.60}$$

It is easy to verify that the analytical solution of (13.60) is given by

$$X_t = X_0 \exp\left((\lambda - 0.5\mu^2)t + \mu W_t\right). \tag{13.61}$$

The exact solution (13.61) is also used to evaluate the expected error function at time t_n as

$$\mathcal{E} = \sqrt{E\Big(\sup_{0\le t_n\le 1} (X_{t_n} - Y_n)^2\Big)},$$

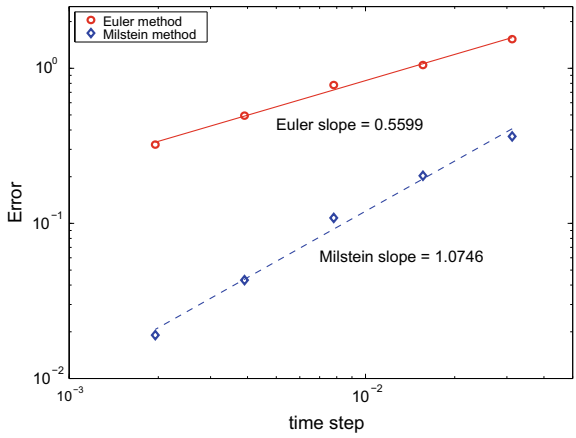

Fig. 13.2 Error plots for the linear equation at time $t = 1$

where X_{t_n} and Y_n are the exact and numerical solutions at time t_n, respectively. In our computations we use $\lambda = -1$, $\mu = 2$, $x_0 = 1$ and simulations are stopped at time $t_n = 1$. In Fig. 13.2 we display the error norms for the Milstein and Euler schemes using five uniform step sizes 2^{-5}, 2^{-6}, 2^{-7}, 2^{-8} and 2^{-9} at the considered time. A logarithmic scale is used on the x- and y-axis. It is clear that decreasing the time step size results in a decrease of errors in both schemes. As expected the Euler method shows a convergence rate of 0.5 whereas the convergence rate of the Milstein method is 1 for this linear stochastic equation.

13.4.2 A Stochastic Linear System

Next we solve the following two-dimensional stochastic system

$$dX_t = a(t, X_t)dt + b(t, X_t)dW_t, \tag{13.62}$$

where $X_t = \left(X_t^1, X_t^2\right)^T$ is the unknown vector. The drift vector $a(t, X_t)$ and the diffusion matrix $b(t, X_t)$ are given as

$$a(t, X_t) = \begin{pmatrix} -\lambda & \lambda \\ \lambda & -\lambda \end{pmatrix} X_t, \qquad b(t, X_t) = \begin{pmatrix} \mu & 0 \\ 0 & \mu \end{pmatrix} X_t.$$

The analytical solution of this system is given by [20]

$$X_t = P \begin{pmatrix} \exp\left(\rho^+(t)\right) & 0 \\ 0 & \exp\left(\rho^-(t)\right) \end{pmatrix} P^{-1} X_0,$$

where $\rho^{\pm}(t) = (-\lambda - 0.5\mu^2 \pm \lambda)t + \mu W_t$,

$$P = \frac{1}{\sqrt{2}} \begin{pmatrix} 1 & 1 \\ 1 & -1 \end{pmatrix} \quad \text{and} \quad X_0 = \begin{pmatrix} 1 \\ 2 \end{pmatrix}.$$

In all results presented for the system (13.62) we used $\lambda = 1$, $\mu = 2$ and different time steps. In Fig. 13.3 we display the difference between the simulated solution and analytical solution at time $t_n = 1$ using the Euler method. The obtained results for the Milstein method are depicted in Fig. 13.4. For a clear presentation a decimal logarithmic scale is used on the y-axis. It is evident that for both component the errors computed using the Milstein scheme show different trends than those computed using the Euler scheme. For all selected time steps, the Milstein scheme is more accurate than the Euler scheme for this linear system. To further quantify the errors in the Milstein and Euler schemes, we calculate the following errors

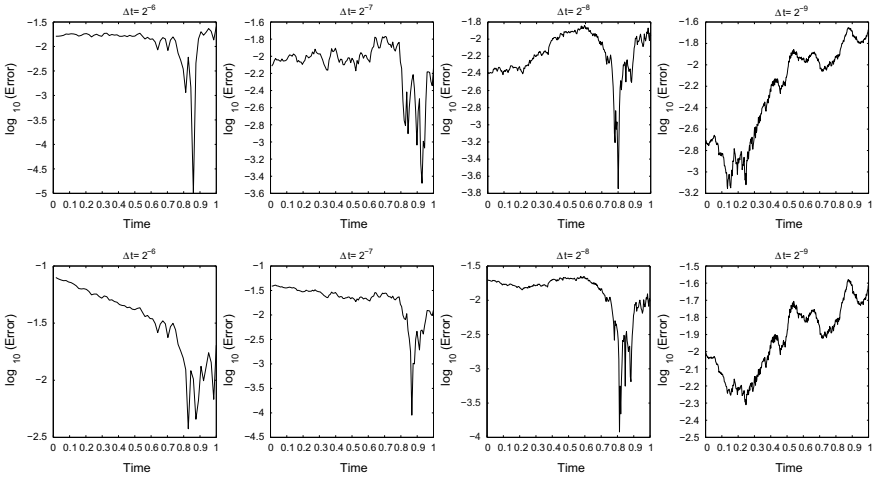

Fig. 13.3 Errors in the solution X_t^1 (first row) and the solution X_t^2 (second row) at time $t_n = 1$ obtained using the Euler scheme

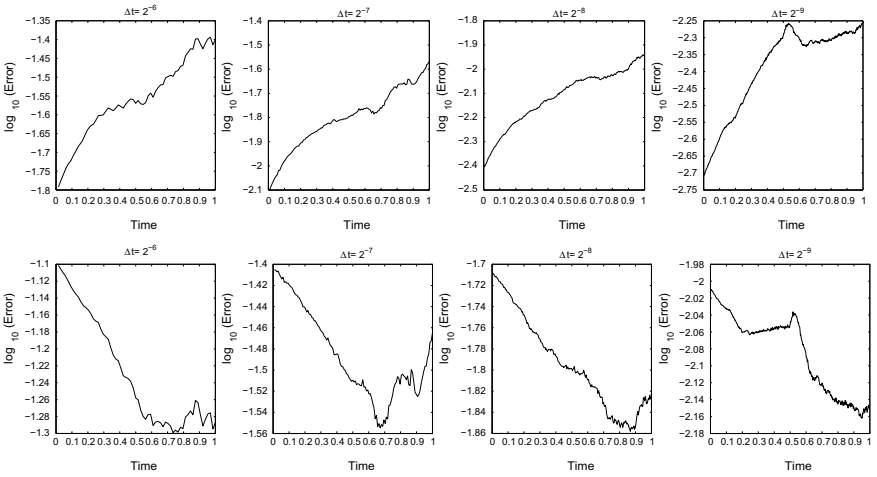

Fig. 13.4 Errors in the solution X_t^1 (first row) and the solution X_t^2 (second row) at time $t_n = 1$ obtained using the Milstein scheme

$$\mathcal{E}_1 = \left|E(X_{t_n}^k) - E(Y_n^i)\right|, \qquad \mathcal{E}_2 = \sqrt{\left(E\left(X_{t_n}^k - Y_n^k\right)^2\right)}, \qquad k = 1, 2,$$

where $X_{t_n}^k$ and Y_n^k are the exact and numerical solutions at time t_n, respectively.

In Table 13.1 we summarize the obtained results for different time steps. A simple inspection of this table reveals that a decay of all considered errors is achieved by decreasing the time steps for both solutions X_t^1 and X_t^2. However, a faster decay

Table 13.1 Errors $\mathcal{E}_1$ and $\mathcal{E}_2$ for the linear system at time $t_n = 1$ using different time steps

	Milstein method				Euler method			
	X_t^1		X_t^2		X_t^1		X_t^2	
Δt	$\mathcal{E}_1$	$\mathcal{E}_2$	$\mathcal{E}_1$	$\mathcal{E}_2$	$\mathcal{E}_1$	$\mathcal{E}_2$	$\mathcal{E}_1$	$\mathcal{E}_2$
2^{-5}	0.65E-1	0.14E-0	0.13E-0	0.22E-0	0.63E-1	0.19E+1	0.63E-1	0.28E+1
2^{-6}	0.28E-1	0.47E-1	0.59E-1	0.62E-1	0.95E-2	0.12E+1	0.95E-2	0.16E+1
2^{-7}	0.16E-1	0.14E-1	0.32E-1	0.17E-1	0.84E-2	0.47E-0	0.84E-2	0.64E-0
2^{-8}	0.78E-2	0.12E-2	0.16E-1	0.19E-2	0.46E-2	0.17E-0	0.46E-2	0.24E-0
2^{-9}	0.42E-2	0.06E-2	0.82E-2	0.09E-2	0.83E-2	0.13E-0	0.83E-2	0.18E-0

has been observed in the errors computed using the Milstein scheme. Again, the Milstein method shows a first-order accuracy for this linear system. Hence, our next computations are realized with the Milstein scheme only. It should be stressed that, in our simulations the computational times required for the Milstein scheme is about 1.5 times the computational time needed for the Euler scheme. It may be noted that 10, 000 realizations were sufficient for a weak convergence of the computations. The CPU times must be taken as indicative since the absolute numbers can vary with the state and configuration of the operating system.

13.4.3 Numerical Solution of the Stochastic Prebiotic System

Now, we turn our attention to the stochastic prebiotic system (13.2). We present numerical simulations for the prototype model sketched in Fig. 13.1. The model accounted for four catalyzed selfreplicator species along with an activated and inactivated residues. The kinetic rates $(k_{ij})_{1\leq i,j\leq 4}$ are entries of the following matrix:

$$\mathbf{K} = \begin{pmatrix} K_1 \\ K_2 \\ K_3 \\ K_4 \end{pmatrix} = \begin{pmatrix} 0.5 & 1.6 & 0.0 & 2.2 \\ 1.5 & 1.0 & 2.0 & 0.0 \\ 0.5 & 0.0 & 0.6 & 0.4 \\ 0.1 & 0.0 & 0.0 & 0.0 \end{pmatrix}, \tag{13.63}$$

where K_i for $i = 1, \ldots, 4$, denote the row vectors of the matrix $\mathbf{K}$. The remaining coefficients are set to $\gamma = 1, \alpha_i = 1$ and $\delta_i = 0.1$ for $i = 1, \ldots, 4$. Initial conditions are randomly chosen in such a way that the concentration of the sum of all the species is equal and arbitrarily fixed as 1, i.e.

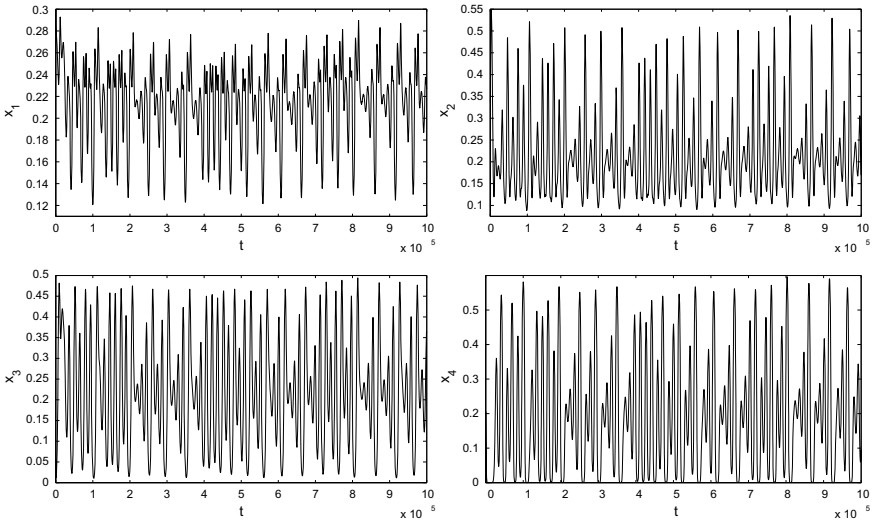

Fig. 13.5 Time series for the four catalyzed species in the test case with additive noise

$$\sum_{i=1}^{4} x_{i,t_0} + y_{t_0} + z_{t_0} = 1.$$

Two physical stochastic excitations are used: stochastic forces driven by additive noise, that mimic a vast prebiotic scenario in which the mean effects of the medium are negligible, and stochastic forces driven by multiplicative noise, which would arise in a scenario when there is interchange of material with the surroundings. In all our simulations presented, the time step is fixed to $\Delta t = 0.1$ and the obtained results are displayed at time $t = 10^6$.

First, we consider the case with additive noise. Thus, the diffusion matrix in the system (13.3) is a 6×6-matrix given by

$$\mathcal{G}(t, \mathbf{X}(t)) = \sigma \begin{pmatrix} \mathbf{K} & \mathbf{0} \\ \mathbf{0} & \mathbf{0} \end{pmatrix}, \tag{13.64}$$

where $\mathbf{K}$ is the kinetic matrix given in (13.63) and σ is a parameter fixed in our simulations to $\sigma = 10^{-2}$. In Fig. 13.5 we display time series for the four catalyzed selfreplicator species. Using these series, global attractors are illustrated in Fig. 13.6. From the obtained time series we see an important contribution of frequencies that correspond to high order periods. This fact is a consequence of the coexistence of different attractors such as chaos, chaotic bands and fixed points (which appear perturbed by the stochastic excitation). Note that the contribution of the stochastic perturbation to the time series and chaotic attractors is evident through the different frequencies that correspond to high order periods. It is interesting to remark that

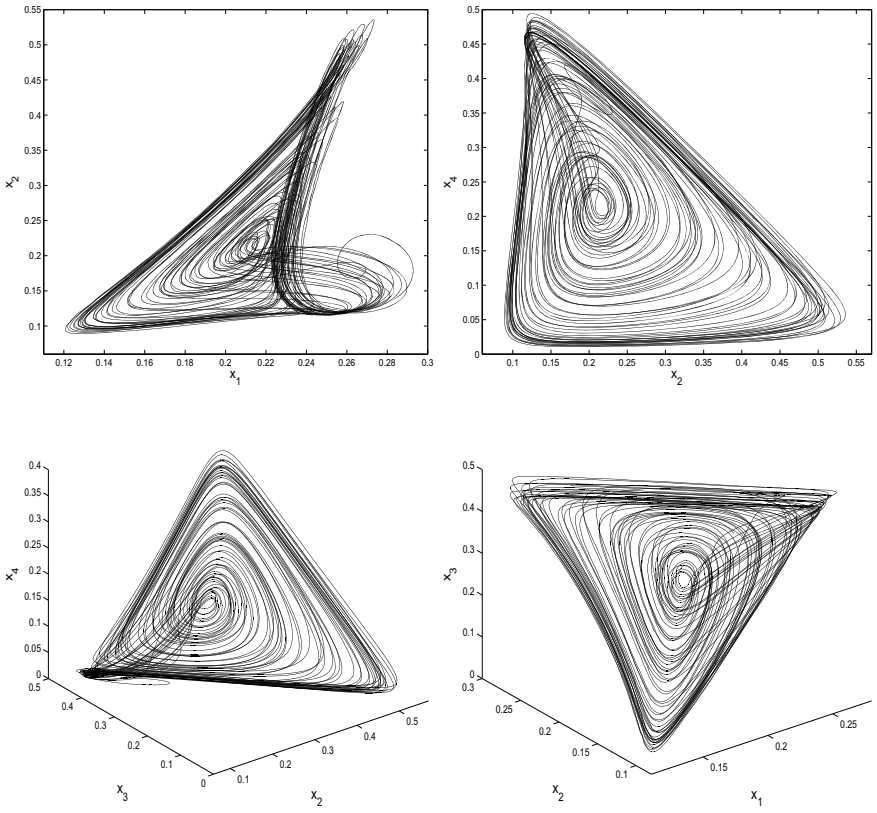

Fig. 13.6 Consecutive global attractors obtained for the four catalyzed species in the test case with additive noise

some fluctuations are present in the attractors shown in Fig. 13.6. These fluctuations are due to the presence of stochastic terms in the system (13.2) and can be reduced either by decreasing the stochastic amplitude σ in (13.64) or increasing the number of realizations used for constructing mean solutions.

It should be pointed out that, the deterministic dynamics of this model (obtained after removing the stochastic terms by setting $\sigma = 0$) has already been analyzed in a relevant but restricted situation, a system formed by cyclically linked species (a hypercycle) in [8, 15]. Perhaps, the most relevant property of this special network is that it allows the coexistence of all species involved in the organization. Moreover, whereas for networks formed by less than four species the fixed point of coexistence is asymptotically stable, for networks larger than four, this fixed point becomes unstable appearing surrounded by a cyclic limit. This fact has special significance when the stochastic process is taken into account in the model as can be seen from the results presented in Fig. 13.6.

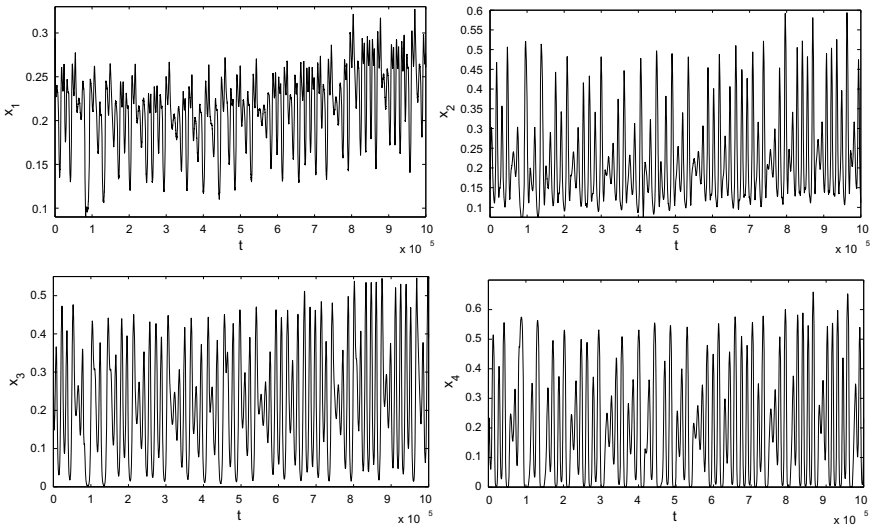

Fig. 13.7 Time series for the four catalyzed species in the test case with multiplicative noise

Finally, we consider the case with a multiplicative noise given by the following diffusion 6×6-matrix in (13.3)

$$\mathcal{G}(t, \mathbf{X}(t)) = \sigma \begin{pmatrix} K_1\mathcal{X}(t) & 0 & 0 & 0 & 0 & 0 \\ 0 & K_2\mathcal{X}(t) & 0 & 0 & 0 & 0 \\ 0 & 0 & K_3\mathcal{X}(t) & 0 & 0 & 0 \\ 0 & 0 & 0 & K_4\mathcal{X}(t) & 0 & 0 \\ 0 & 0 & 0 & 0 & 0 & 0 \\ 0 & 0 & 0 & 0 & 0 & 0 \end{pmatrix}, \tag{13.65}$$

where $\mathcal{X}(t) = (x_1(t), x_2(t), \ldots, x_N(t))^T$ and K_i is the i-th row of the matrix $\mathbf{K}$ in (13.63). Note that, unlike the previous test case, the considered case is a problem coupled in nature with strong stochastic perturbation and therefore, good numerical accuracy is required in order to capture the different phenomena present in its evolving solution. As a consequence, the later test case is more difficult to handle; the results shown here illustrate the robustness of the Milstein method. Note that for the diffusion matrix (13.65), the double Itô integrals $\int_{0,i\neq j,i,j=1,2}^{\Delta t} W_s^{(i)} W_s^{(j)}$ are non zero in the Milstein method resulting in more computations to be done compared to the case with additive noise (13.64).

Figure 13.7 shows the time series for the four catalyzed selfreplicator species. The associated phase-portraits for the four catalyzed species are illustrated in Fig. 13.8. Formation of complex dynamics can be clearly seen from the presented results. Starting from randomly distributed concentrations, stationary states are reached exhibiting clusters with different scales. We have also observed that the convergence to these

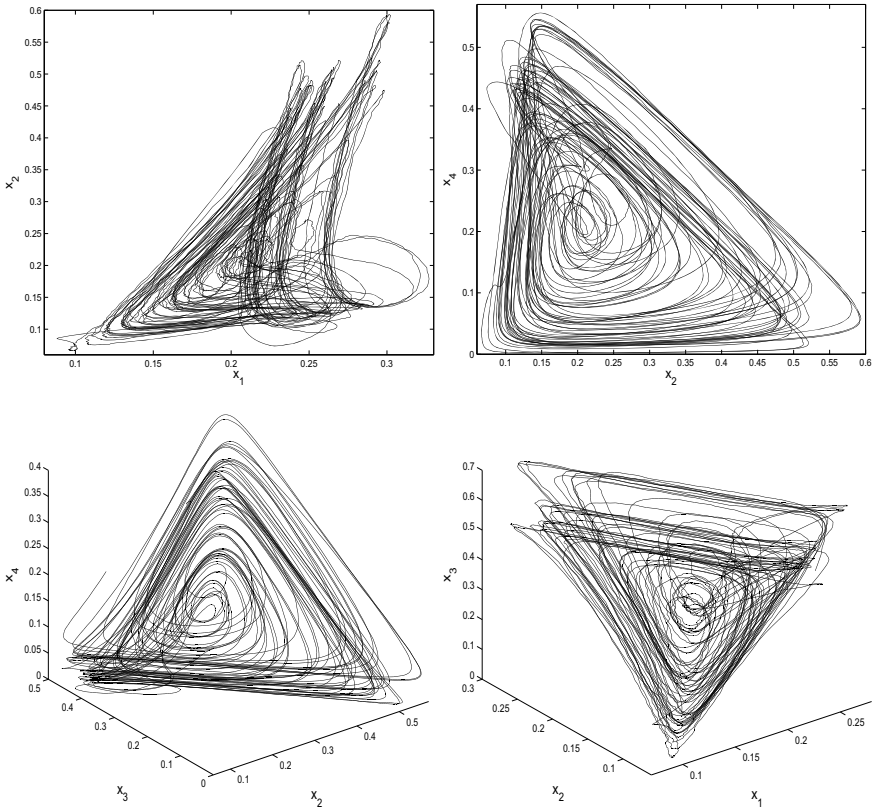

Fig. 13.8 Consecutive global attractors obtained for the four catalyzed species in the test case with multiplicative noise

stationary states depends on the kinetic coefficients and the amplitude of stochastic excitations. We should mention that for the deterministic model, periodically distributed aggregates appear in the formed dynamics. However, for the stochastic model, this periodicity is broken and regions with a high concentration of replicators are separated from lower concentration ones, and the boundaries between the clusters remain almost constant in time. Formally, the Hop bifurcation can be investigated by analyzing the six eigenvalues of the linearization at zero as functions of the parameter α_i. In the considered stochastic case the analysis is rather complicated. Indeed, the above mentioned eigenvalues need to be replaced by the Lyapunov exponents of the stochastic system (13.2). In this case the origin remains as a stable fixed point as long as the first Lyapunov exponent λ_1 (as a function of the bifurcation parameter α_i) be negative. Hence, stability is lost when λ_1 becomes positive and six different qualitative behavior emerges, which depends on the sign of the other five Lyapunov exponents. Finally, the results presented in this study strengthen the hypothesis of a prebiotic scenario with stochastic reactions where all the metabolic necessities were

carried out by RNA-like molecules. However, it is not clear where and when these stochastic excitations should be implemented in the kinetic reactions since no experimental information is provided regarding these issues. Further investigations are therefore, required to give an explanation to the origin of cellular structures.

References

1. Abdulle A, Pavliotis GA (2012) Numerical methods for stochastic partial differential equations with multiple scales. J Comput Phys 231(6):2482–2497
2. Almeida RC, Oden JT (2010) Solution verification, goal-oriented adaptive methods for stochastic advection-diffusion problems. Comput Methods Appl Mech Eng 199(37–40):2472–2486
3. Angstmann CN, Donnelly IC, Henry BI, Jacobs B, Langlands TA, Nichols JA (2016) From stochastic processes to numerical methods: a new scheme for solving reaction subdiffusion fractional partial differential equations. J Comput Phys 307:508–534
4. Chacón P, Nuno J (1995) Spatial dynamics of a model for prebiotic evolution. Phys D: Nonlinear Phenom 81(4):398–410
5. Chekroun MD, Park E, Temam R (2016) The stampacchia maximum principle for stochastic partial differential equations and applications. J Differ Equ 260(3):2926–2972
6. Company R, Ponsoda E, Romero JV, Roselló MD (2009) A second order numerical method for solving advection-diffusion models. Math Comput Model 50(5–6):806–811
7. Doudna JA, Szostak JW (1989) RNA-catalysed synthesis of complementary-strand RNA. Nature 339(6225):519
8. Eigen M, Schuster P (1982) Sigmund, from biological macro-molecules to protocells: the principle of early evolution. Springer, Berlin
9. Eigen M, Schuster P (1979) The hypercycle, a principle of natural self-organization. Springer, New York
10. El-Amrani M, Seaid M, Zahri M (2012) A stabilized finite element method for stochastic incompressible navier-stokes equations. Int J Comput Math 89(18):2576–2602
11. Forst CV (1996) Chaotic interactions of self-replicating RNA. Comput Chem 20(1):69–83
12. Ghanem RG, Spanos PD (1991) Stochastic finite elements: a spectral approach. Springer, New York
13. Giletti T (2011) Traveling waves for a reaction-diffusion-advection system with interior or boundary losses. Comptes Rendus Math 349(9–10):535–539
14. Gropp W, Smith B (1993) Scalable, extensible, and portable numerical libraries. In: Proceedings of scalable parallel libraries conference. IEEE, pp 87–93
15. Hofbauer J, Schuster P (1984) Dynamics of linear and nonlinear autocatalysis and competition in stochastic phenomena and chaotic behavior in complex systems. Springer, Berlin
16. Itô K (1944) Stochastic integral. Proc Imp Acad 20(8):519–524
17. Itô K (1951) Multiple wiener integral. J Math Soc Jpn 3(1):157–169
18. Jentzen A, Kloeden PE (2011) Taylor approximations for stochastic partial differential equations, vol 83. SIAM, Philadelphia
19. Karatzas I, Shreve SE (1998) Brownian motion and stochastic calculus, 2nd edn. Graduate texts in mathematicals. Springer, New York. http://cds.cern.ch/record/396069
20. Klöden PE, Platen E (1992) Numerical solution of stochastic differential equations. Springer, Berlin
21. Kloeden P, Platen E (1999) The numerical solution of stochastic differential equations. Springer, Berlin
22. Kloeden P, Platen E, Schurz H (1994) Numerical solution of SDE through computer experiments. Springer, Berlin
23. Mai-Duy N, Tran-Cong T (2008) An efficient domain-decomposition pseudo-spectral method for solving elliptic differential equations. Commun Numer Methods Eng 24(10):795–806

24. Manouzi H, Seaı M, Zahri M et al (2007) Wick-stochastic finite element solution of reaction-diffusion problems. J Comput Appl Math 203(2):516–532
25. Mathew T (2008) Domain decomposition methods for the numerical solution of partial differential equations, vol 61. Springer Science & Business Media
26. Milstein G (1995) Numerical integration of stochastic differential equations. Kluwer Akademic Publishers, Dordrecht
27. Milstein G, Tretyakov MV (2016) Layer methods for stochastic navier-stokes equations using simplest characteristics. J Comput Appl Math 302:1–23
28. Milstein GN, Tretyakov MV (2004) Stochastic numerics for mathematical physics. Springer, Berlin
29. Mohamed K, Seaid M, Zahri M (2013) A finite volume method for scalar conservation laws with stochastic time-space dependent flux functions. J Comput Appl Math 237(1):614–632
30. Narayanan VAB, Zabaras N (2005) Variational multiscale stabilized fem formulations for transport equations: stochastic advection-diffusion and incompressible stochastic navier-stokes equations. J Comput Phys 202(1):94–133
31. Nishikawa H (2010) A first-order system approach for diffusion equation. ii: unification of advection and diffusion. J Comput Phys 229(11):3989–4016
32. Nuño JC, Chacón P, Moreno A, Morán F (1995) Compartimentation in replicator models. In: Proceedings of the 3rd European conference on advances in artificial life. Springer, London, UK, pp 116–127
33. Quarteroni A, Valli A (1999) Domain decomposition methods for partial differential equations. Oxford University Press, Oxford
34. Quarteroni A, Veneziani A, Zunino P (2002) A domain decomposition method for advection-diffusion processes with application to blood solutes. SIAM J Sci Comput 23(6):1959–1980
35. Rößler A, Seaïd M, Zahri M (2008) Method of lines for stochastic boundary-value problems with additive noise. Appl Math Comput 199(1):301–314
36. Rößler A, Seaïd M, Zahri M (2009) Numerical simulation of stochastic replicator models in catalyzed RNA-like polymers. Math Comput Simul 79(12):3577–3586
37. Schiesser W (1991) The numerical method of lines: integration of partial differential equations. Academic Press, Cambridge
38. Smith B, Bjorstad P, Gropp W (2004) Domain decomposition: parallel multilevel methods for elliptic partial differential equations. Cambridge University Press, Cambridge
39. Smith BF, Widlund OB (1990) A domain decomposition algorithm using a hierarchical basis. SIAM J Sci Stat Comput 11(6):1212–1220
40. Tveito AMBA, Bruaset AM (2006) Numerical solution of partial differential equations on parallel computers. Springer, Berlin
41. Verwer JG, Sanz-Serna JM (1984) Convergence of method of lines approximations to partial differential equations. Computing 33(3–4):297–313
42. Zafarullah A (1970) Application of the method of lines to parabolic partial differential equations with error estimates. J ACM (JACM) 17(2):294–302
43. Zahri M (2010) Numerical solution of a stochastic lorenz attractor. J Num Mat Stoch 2:1–11
44. Zahri M (2014) Multidimensional milstein scheme for solving a stochastic model for prebiotic evolution. J Taibah Univ Sci 8(2):186–198
45. Zahri M (2018) Barycentric interpolation of interface solution for solving stochastic partial differential equations on non-overlapping subdomains with additive multi-noises. Int J Comput Math 95(4):645–685
46. Zahri M, Al Madinah K (2012) On numerical schemes for solving a stochastic advection-diffusion. Int J Pure Appl Math 77(5):681–694
47. Zahri M, Seaïd M, Manouzi H, El-Amrani M (2005) Wiener-itô chaos expansions and finite-volume solution of stochastic advection equations. Finite volumes for complex applications IV. ISTE, London, pp 525–538